

# Record heating in magnetic hyperthermia of metallic iron nanocubes and way for further improvements.

B. Mehdaoui, A. Meffre, L.-M. Lacroix, J. Carrey\*, S. Lachaize, M. Respaud

Université de Toulouse; INSA; UPS; LPCNO (Laboratoire de Physique et Chimie des Nano-Objets), 135 avenue de Rangueil, F-31077 Toulouse, France and  
CNRS; UMR 5215 ; LPCNO, F-31077 Toulouse, France

M. Gougeon

Institut CARNOT - CIRIMAT - UMR 5085, Bâtiment 2R1, 118 route de Narbonne  
F-31062 Toulouse, France

B. Chaudret

Laboratoire de Chimie de Coordination-CNRS, 205 rte de Narbonne, 31077 Toulouse cedex 4,  
France

## Abstract:

In magnetic hyperthermia, improving the heating properties of nanoparticles above those of iron oxides requires high magnetization materials and a fine tuning of their size. We report the hyperthermia properties of chemically synthesized metallic Fe nanocubes displaying the bulk magnetization. Their losses reach the record value of  $5.6 \pm 0.5$  mJ/g, largely exceeding values reported in other systems. We discuss these preliminary results and propose some guidelines to tailor their hysteresis loops to further increase their efficiency.

## Main Text:

In oncology, hyperthermia is a way to improve the efficiency of chemotherapy [1] or radiotherapy [2] by raising the temperature of a tumour to 41-45 °C during a few hours. To achieve this goal, one possibility called magnetic hyperthermia consists in using magnetic nanoparticles (MNPs): MNPs are first localised inside the tumour and then excited by an alternating magnetic field of moderate amplitude  $\mu_0 H_{app}$  (12-25 mT) at a frequency  $f_{exc}$  in the range 100-400 kHz [3]. The power released by the NPs is assessed by their specific absorption rate (SAR) or their losses  $A$ , related by the equation  $SAR = Af_{exc}$ . Exploiting this effect in oncology requires biocompatible MNPs displaying high SARs. In particular, high SARs would open the possibility to treat smaller size tumours [4]. Hergt *et al.* estimated that MNPs with SARs above 1 kW/g could efficiently treat 3 mm diameter tumours, a size which constitutes so far the bottom limit for their detection and for an intra-tumoral injection. Also, such SAR values could open the way to treatments based on a systemic injection of targeted NPs, which would improve

their distribution inside the tumour and avoid the surgical procedure required for an intra-tumoral injection [4].

Maximizing the SAR above the 1 kW/g limit is a real challenge. Note first that human body cannot be exposed to alternating magnetic field when the  $H_{app}f_{exc}$  product is above a given value [4]. The most favourable case when i) the magnetization loop, characterized by a coercive field  $H_C$  and a saturation magnetization per unit mass  $\sigma_S$ , is perfectly square ii)  $H_{app} \approx H_C$ , leads to  $SAR_{max} = 4\mu_0\sigma_S H_{app}f_{exc}$ . Unfortunately, due to random orientations of easy axis, magnetic interactions and thermal activation, hysteresis loops of MNPs assemblies are far from being square. More generally, one can write:

$$SAR = 4\alpha\mu_0\sigma_S H_{app}f_{exc} \quad (1)$$

where  $\alpha$  is a dimensionless parameter which characterizes the relative area of the hysteresis loops with respect to the ideal square. A consequence of Equ. (1) and of the limitation of the  $H_{app}f_{exc}$  product is that maximising the SAR requires MNPs displaying a high  $\sigma_S$  and hysteresis loops as square as possible (large  $\alpha$ ). High magnetization materials are essentially Ni, Fe, Co and their alloys. Among them, metallic Fe is the most promising one since it displays a very large  $\sigma_S$  and is *a priori* the most biocompatible.

However, so far, the most widely studied materials for magnetic hyperthermia have been the iron oxides, because of their full biocompatibility and the relative simplicity of their synthesis. Optimized chemically-synthesized  $Fe_3O_4$  NPs have shown losses up to 1.5 mJ/g at 400 kHz [5]. Among high magnetization materials, higher loss values up to 3.2 mJ/g at 400 kHz have been reported for Co MNPs [6]. The scarce results published so far on Fe MNPs are disappointing, as a consequence of the lack of control of the surface oxidation: hyperthermia experiments were performed on  $Fe/Fe_xO_y$  core-shell MNPs which displayed low  $\sigma_S$  and losses comparable to those measured on iron oxides [7].

In this paper we focus on a preliminary study of fully metallic ferromagnetic Fe MNPs. Our group has developed an organometallic synthesis allowing the controlled synthesis of pure iron NPs displaying the bulk magnetization [8,9,10]. We report in this article the magnetic and hyperthermia measurements on ferromagnetic 11 and 16 nm nanocubes. The 16 nm nanocubes display SAR values reaching up to  $1690 \pm 160$  W/g at 300 kHz and 66 mT, corresponding to losses of  $5.6 \pm 0.5$  mJ/g, which are the highest reported in the literature. These results are discussed aiming at defining the way toward a better performance, based on the size-dependence of the coercive field in single-domain MNPs.

**Synthesis and characterization.** The two samples of Fe nanocubes were synthesized by a two steps organometallic route which has been previously described [10]. A complete description of the size and shape control on iron NPs synthesized by this route will be published elsewhere. First, we prepared small Fe seeds (~2 nm) by decomposition at 150°C for 24h of a mesitylene (20mL) solution of the iron dimer  $\{Fe[N(SiMe_3)_2]_2\}_2$ , (376 mg, 0.5 mmol) under 3 bars of  $H_2$  in a Fisher-Porter bottle (170mL) [11]. In a second time, a mixture of hexadecylammonium chloride and hexadecylamine was added to the colloidal solution. For sample **1**, the ratio ammonium/amine was 1:2 (277 mg, 1 mmol hexadecylammonium chloride, 483 mg, 2 mmols hexadecylamine). For sample **2**, this ratio was 1.1:2 (304.7 mg, 1.1 mmol

hexadecylammonium chloride, 483 mg, 2 mmols hexadecylamine). The solution was stirred for 20 minutes at 90°C then pressurised under 3 bars of H<sub>2</sub> and heated at 150°C. After 48h, a black precipitate was formed at the bottom of the Fisher-Porter bottle. The solvent was filtered off and the precipitate washed three times with 15 mL of toluene to remove the surfactants in excess and other remaining molecular species. The final iron content was 71 % and 88 % for samples **1** and **2**, respectively, as determined by chemical analysis.

The nanocubes were then characterized by transmission electron microscopy (TEM) on a JEOL 1011 microscope for a bright-field transmission electronic microscopy or on a JEOL-2100F field-emission microscope for high-resolution TEM (HRTEM). Microscopy samples were prepared by the deposition of a drop of diluted colloidal solution onto a carbon-coated copper grid. The HRTEM observation shown in Fig. 1 revealed that the nanocubes were single-crystalline and exhibited a bcc crystal structure, with facets of (100) planes. A thin oxide shell surrounds the bcc Fe core due to a partial oxidation during the transfer into the microscope [see Fig. 1(a)]. SQUID measurement however confirmed that no significant oxidation occurred during the synthesis (see below). Most of the nanocubes were embedded in organic mesophases as revealed by TEM micrographs [see Figs. 1(b) and 1(c)], in agreement with the reaction medium composition. Such nanocube-filled mesophases have already been characterized for a similar system in which carboxylic acid was used instead of ammonium chloride [8]. Size distributions measured from several TEM micrographs showed that sample **1** and **2** were composed of iron nanocubes of mean side lengths  $16.3 \pm 1.5$  nm (sample **1**) and  $11.3 \pm 1.3$  nm (sample **2**) respectively [see insets of Figs. 1(b) and 1(c)].

Samples for magnetic measurements were prepared and sealed inside the glove box in order to preserve the metallic character of Fe. SQUID measurements on powders of **1** and **2** showed that their saturation magnetizations per unit mass  $\sigma_s$  were  $208 \pm 11$  Am<sup>2</sup>/kg and  $183 \pm 9$  Am<sup>2</sup>/kg at 2 K, and  $200 \pm 10$  Am<sup>2</sup>/kg and  $178 \pm 9$  Am<sup>2</sup>/kg at 300 K, respectively, just below the bulk value. An enlarged view of the hysteresis loop at 300 K for each sample is shown in Fig. 2. Their coercive fields  $H_C$  at 300 K are 16 and 5 mT, respectively.

**Hyperthermia measurements.** Hyperthermia experiments were performed on an induction oven working at a fixed frequency of 300 kHz and a maximum magnetic field of 66 mT. The latter was calibrated using a pick-up coil. For hyperthermia measurements, an ampoule containing the colloidal solution was sealed under vacuum to prevent any oxidation of the NPs. A typical ampoule contains approximately 9 mg of powder and 550 mg of mesitylene. The ampoule was then placed into a calorimeter with 1.5 mL of deionised water, the temperature of which was measured. The measurement time was varied between 20 and 200 seconds, depending on the experimental parameters, so that the temperature rise never exceeds 20°C. For measurements longer than 20 s, the SAR values were corrected from the calorimeter losses. The temperature rise at the end of the magnetic field application was always measured after having homogenized quickly the temperature inside the calorimeter. The homogeneity was checked by putting two probes at the top and the bottom of the calorimeter. The SAR values at 66 mT and their error bars were obtained by averaging three measurements on three different ampoules arising from the same synthesis (9 values). The complete magnetic-field dependence of the SAR was measured on a single ampoule for each synthesis and its SAR values renormalized accordingly. The magnetic-field dependence in the range of the coercive field (see below) was however measured on the six

ampoules to ensure that the observed difference between sample **1** and **2** was not due to an ampoule-to-ampoule variation.

During hyperthermia experiments, the spatial organisation of the MNPs in the vessel was completely redistributed by the application of the magnetic field. Indeed, while the MNPs falls down by gravity at the bottom of the ampoule in the absence of applied magnetic field, the MNPs formed small spikes in the direction of the field when a small magnetic field was applied. Moreover, for larger magnetic fields, the MNPs self-organized into regularly spaced needles, which disintegrated as soon as the magnetic field was stopped. A video-extracted picture illustrating this phenomenon in sample **1** is shown in Fig. 3(a). The video is available as a Web Enhanced Object. The magnetic field for which these needles formed was higher for sample **1** than for sample **2** and ranged between 20 to 30 mT.

Fig. 3(b) displays the extracted SAR values measured at 300 kHz as a function of the applied magnetic field for the two samples. In both cases, SAR increases strongly in the range 10-30 mT and follows a roughly linear increase above without complete saturation. For sample **1**, the increase is sharper and occurs for a higher magnetic field than for sample **2**. Such an abrupt increase followed by a plateau is a typical feature of ferromagnetic samples and was previously reported on ferromagnetic FeCo MNPs [12] : the sharp rise of the SAR occurs as  $H_{app}$  reaches the coercive field of the MNPs. SARs reach large values up to  $1690 \pm 160$  W/g and  $1320 \pm 140$  W/g at 66 mT for sample **1** and **2**, respectively. For sample **1**, this value corresponds to losses of  $5.6 \pm 0.5$  mJ/g. They are the highest reported so far and exceed by a factor 3 the values reported on optimized chemically-synthesized iron oxide NPs.

**A need for further improvements.** Calculating the value of  $\alpha$  from Equ. (1) gives an estimate of the efficiency of any system with respect to hyperthermia applications. In our case, the calculation of  $\alpha$  at  $H_{app} = 66$  mT using measured  $\sigma_S$  at 300 K leads to 0.11 and 0.09 for samples **1** and **2**, respectively. We argue that the presence of magnetic interactions is the main reason for these low  $\alpha$  values. In the case of the Stoner-Wohlfarth (SW) model and considering that i) the MNPs have 3-D randomly distributed anisotropy axis, ii) the MNPs are magnetically independent, iii) the effect of temperature on the magnetization reversal process is neglected and iv) the MNPs do not physically rotate in the magnetic field (no Brownian motion),  $\alpha_{SW}$  equals 0.25, assuming that  $H_{app} = 2H_C$  [13]. The analysis of Monte-Carlo simulations indicates that  $\alpha_{SW}$  is not modified when a finite temperature and frequency partially decrease the coercive field [14] (see below). A  $\alpha$  value of 0.3 has been measured on randomly oriented optimized iron oxide NPs [5], evidencing that reaching  $\alpha_{SW}$  is a reasonable experimental expectation and that the efficiency of our system could be further improved.

When magnetic interactions become non negligible, it is now well admitted that both  $H_C$  and  $M_R$  decrease [15], thus reducing  $\alpha$  compared to the Stoner-Wohlfarth theoretical value. The presence of magnetic interactions in our samples is obvious from several observations: i) the nanoparticles form dense needles when the magnetic field is on; even in the absence of magnetic field, they form a precipitate at the bottom of the vessel. ii) In SQUID measurements, the  $M_R/M_S$  ratio ( $M_R$  is the remnant magnetization and  $M_S$  the saturation magnetization) is 0.2 and 0.06 for samples **1** and **2**, respectively, whereas 0.5 is expected in the absence of interactions (see Fig. 2). iii) The saturation field is well above  $2H_C$  (see Fig. 2).

A second improvement of our system would concern the working magnetic field. Here, huge losses have been measured at a magnetic field of 66 mT whereas only magnetic field close to 20 mT can be applied in a medical hyperthermia treatment setup [16]. Thus optimized iron NPs for hyperthermia applications should display both a reduced saturation field and an enhanced  $\alpha$  value.

**Using size to tune the coercive field.** To achieve these goals, it is first of all necessary to use colloidal solutions of MNPs where the magnetic interactions are less effective, which will increase  $\alpha$ . Given that, the coercive field of MNPs can be adjusted through their size. Indeed, we recently reported that  $\mu_0 H_C$  can be satisfactorily described by an extended Stoner-Wohlfarth model and reads [12, 17, 18]:

$$\mu_0 H_C = \frac{2K}{\rho\sigma_s} \left[ 0.479 - 0.81 \left( \frac{k_B T}{2KV} (\ln 1/f_{exc} \tau_0) \right)^{\frac{3}{4}} \right],$$

where  $V$  is the MNP volume,  $K$  their anisotropy,  $\rho$  their density and  $\tau_0 = 10^{-9}$  s. Targeting  $H_C=10$  mT for a working magnetic field of 20 mT at 100 kHz would require MNPs of 14 nm if they display the bulk anisotropy. With an enhanced anisotropy compared to the bulk, this optimal size should be reduced accordingly. A supplementary condition is that the MNPs should not rotate in the magnetic field by Brownian motion, which would reduce  $\alpha$ . This requires that  $V > \frac{k_B T}{3\eta f_{exc}}$ ,

where  $\eta$  is the viscosity of the medium. This leads to a hydrodynamic NP diameter above 15 nm, using the viscosity of water. In future *in-vivo* applications, the iron magnetic cores should be surrounded with layers aiming at protecting them from oxidation and ensuring their biodisponibility and targeting. As a matter of fact these layers will also have two additional functions which will increase their efficiency: i) to limit the magnetic interactions between the magnetic NPs and ii) to reduce the influence of Brownian motion. To summarize, these simple arguments indicate that the MNPs studied here will certainly constitute good magnetic cores for future applications once they will be surrounded by additional layers. These non-trivial post-treatments will constitute the future developments of this work.

Our measurements of very large SAR in metallic iron nanoparticles above the 1 kW/g limit confirm the potential of high magnetization MNPs for future hyperthermia applications. Size and coating adjustments should be used to increase their efficiency by controlling their coercive and saturation fields and by suppressing the Brownian motion. The exact optimal size depends on the anisotropy of the synthesized MNPs. This illustrates that hyperthermia applications still require progresses in the synthesis of colloidal solutions of individual coated nanoparticles with varying size and need basic research and detailed measurements on their magnetic properties, especially their anisotropy.

**Acknowledgements:** We acknowledge InNaBioSanté foundation, AO3 program from Université Paul Sabatier (Toulouse) and Conseil Régional de Midi-Pyrénées for financial support, V. Collière (TEMSCAN) for HRTEM, C. Crouzet for technical assistance and A. Mari for magnetic measurements.

## References :

\* Electronic mail : julian.carrey@insa-toulouse.fr

[1] P Wust, B Hildebrandt, G Sreenivasa, B Rau, J Gellermann, H Riess, R Felix, and PM Schlag, *Lancet Oncol.* **3**, 487 (2002)

[2] J. van der Zee, D. González González, G. C van Rhoon, J. D. P. van Dijk, W. L. J. van Putten, A. A. M. Hart, *Lancet* **355**,1119 (2000)

[3] P. Wust, U. Gneveckow, M. Johannsen, D. Böhmer, T. Henkel, F. Kahmann, J. Sehouli, R. Felix, J. Ricke, A. Jordan, *Int. J. Hyperthermia* **22**, 673 (2006)

[4] R. Hergt and S. Dutz, *J. Magn. Magn. Mater.* **311**, 187 (2007)

[5] R. Hergt, R. Hiergeist, I. Hilger, W. A. Kaiser, Y. Lapatnikov, S. Margel and U. Richter, *J. Magn. Magn. Mater.* **270**, 345 (2004)

[6] M. Zeisberger, S. Dutz, R. Müller, R. Hergt, N. Matoussevitch, and H. Bönnehan, *J. Magn. Magn. Mater.* **311**, 224 (2005)

[7] I. Baker, Q. Zeng, W. Li, C. R. Sullivan, *J. Appl. Phys.* **99**, 08H106 (2006)

[8] F. Dumestre, B. Chaudret, C. Amiens, P. Renaud, P. Fejes, *Science* **303**, 821 (2004)

[9] L.-M. Lacroix, S. Lachaize, A. Falqui, M. Respaud and B. Chaudret, *J. Am. Chem. Soc.* **131**, 549 (2009)

[10] E. Snoeck, C. Gatel, L.M. Lacroix, T. Blon, S. Lachaize, J. Carrey, M. Respaud and B. Chaudret, *Nano Lett.* **8**, 4293 (2008)

[11] L-M. Lacroix, S. Lachaize, A. Falqui, T. Blon, J. Carrey, M. Respaud, F. Dumestre, C. Amiens, O. Margeat, B. Chaudret, P. Lecante and E. Snoeck, *J. Appl. Phys.* **103**, 07D521 (2008)

[12] L.-M. Lacroix, R. Bel Malaki, J. Carrey, S. Lachaize, M. Respaud, G. F. Goya and B. Chaudret, *J. Appl. Phys.* **105**, 023911 (2009)

- 
- [13] R. Hergt, W. Andrä, C. G. d'Ambly, I. Hilger, W. A. Kaiser, U. Richter and H.-G. Schmidt, *IEEE Trans. Magn.* **34**, 3745 (1998).
- [14] J. J. Lu, H. L. Huang and I. Klik, *J. Appl. Phys.* **76**, 1726 (1994)
- [15] D. Kechrakos and K. N. Trohidou, *Phys. Rev. B* **58**, 12169 (1998).
- [16] A. Jordan, R. Scholz, K. Maier-Hauff, M. Johannsen, P. Wust, J. Nadobny, H. Schirra, H. Schmidt, S. Deger, S. Loening, W. Lanksch, R. Felix, *J. Magn. Magn. Mater.* **225**, 118 (2001)
- [17] J. Garcia-Otero, A. J. Garcia-Bastida and J. Rivas, *J. Magn. Magn. Mater.* **189**, 377 (1998)
- [18] H. Pfeiffer, *Phys. Stat. Sol. (a)* **120**, 233 (1990)

## Figures

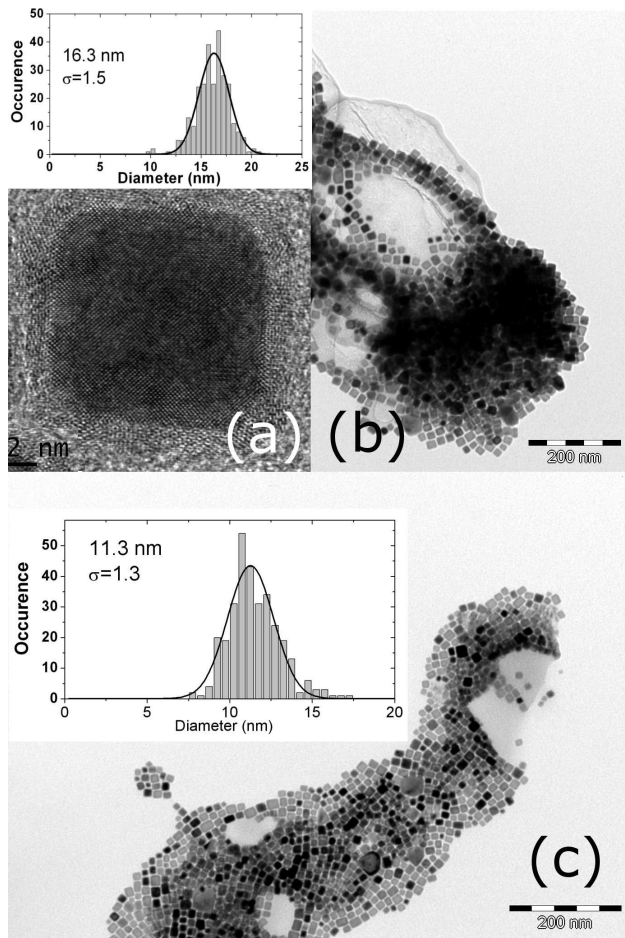


Fig. 1 : TEM micrographs of the iron nanocubes measured in hyperthermia. (a) high-resolution TEM micrograph on an isolated nanocube in sample 1. (b) Sample 1: nanocubes with a mean diameter of 16.3 nm c) Sample 2: nanocubes with a mean diameter of 11 nm. (insets) : nanocube size distribution extracted from the analysis of several TEM micrographs.



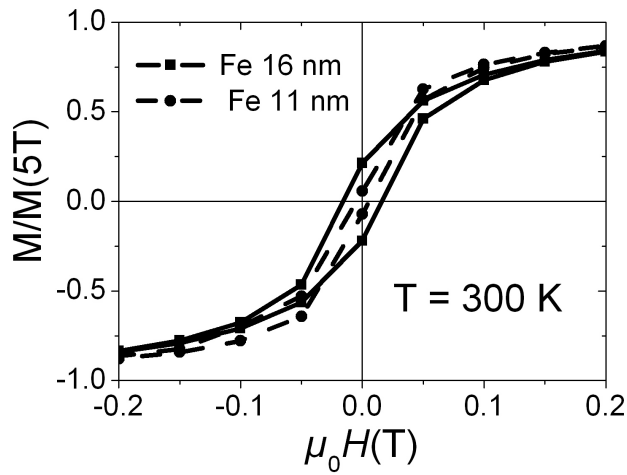


Fig. 2: SQUID measurement at 300 K on Sample 1 (16 nm) and Sample 2 (11 nm). The magnetization is normalized by its value at 5 T.

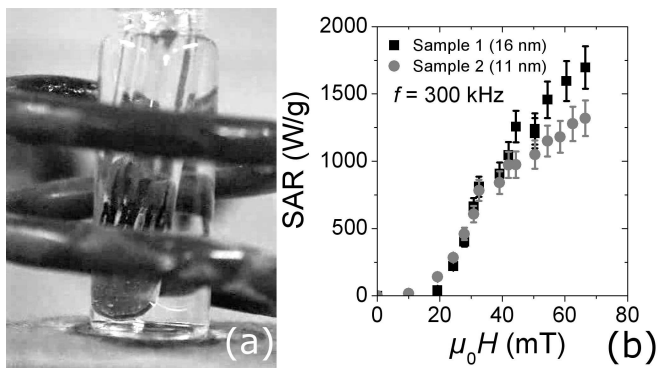


Fig. 3 : (a) Picture extracted from a video showing an hyperthermia experiment on Sample 1 at a magnetic field of 66 mT and 300 kHz, when the field is switched on and then off. On this static image, the field is on. The needles are visible between the two turns of the coil. The full video is available as a Web Enhanced Object (b) Magnetic field dependence of SAR at 300 kHz for the two samples.